SPRINGER PROCEEDINGS IN PHYSICS 120

SPRINGER PROCEEDINGS IN PHYSICS

96 **Electromagnetics in a Complex World**
Editors: I.M. Pinto, V. Galdi, and L.B. Felsen

97 **Fields, Networks, Computational Methods and Systems in Modern Electrodynamics**
A Tribute to Leopold B. Felsen
Editors: P. Russer and M. Mongiardo

98 **Particle Physics and the Universe**
Proceedings of the 9th Adriatic Meeting, Sept. 2003, Dubrovnik
Editors: J. Trampetić and J.Wess

99 **Cosmic Explosions**
On the 10th Anniversary of SN1993J (IAU Colloquium 192)
Editors: J. M. Marcaide and K.W.Weiler

100 **Lasers in the Conservation of Artworks**
LACONA V Proceedings, Osnabrück, Germany, Sept. 15–18, 2003
Editors: K. Dickmann, C. Fotakis, and J.F. Asmus

101 **Progress in Turbulence**
Editors: J. Peinke, A. Kittel, S. Barth, and M. Oberlack

102 **Adaptive Optics for Industry and Medicine**
Proceedings of the 4th International Workshop
Editor: U. Wittrock

103 **Computer Simulation Studies in Condensed-Matter Physics XVII**
Editors: D.P. Landau, S.P. Lewis, and H.-B. Schüttler

104 **Complex Computing-Networks**
Brain-like and Wave-oriented Electrodynamic Algorithms
Editors: I.C. Göknar and L. Sevgi

105 **Computer Simulation Studies in Condensed-Matter Physics XVIII**
Editors: D.P. Landau, S.P. Lewis, and H.-B. Schüttler

106 **Modern Trends in Geomechanics**
Editors: W. Wu and H.S. Yu

107 **Microscopy of Semiconducting Materials**
Proceedings of the 14th Conference, April 11–14, 2005, Oxford, UK
Editors: A.G. Cullis and J.L. Hutchison

108 **Hadron Collider Physics 2005**
Proceedings of the 1st Hadron Collider Physics Symposium, Les Diablerets, Switzerland, July 4–9, 2005
Editors: M. Campanelli, A. Clark, and X. Wu

109 **Progress in Turbulence 2**
Proceedings of the iTi Conference in Turbulence 2005
Editors: M. Oberlack et al.

110 **Nonequilibrium Carrier Dynamics in Semiconductors**
Proceedings of the 14th International Conference, July 25–29, 2005, Chicago, USA
Editors: M. Saraniti, U. Ravaioli

111 **Vibration Problems ICOVP 2005**
Editors: E. Inan, A. Kiris

112 **Experimental Unsaturated Soil Mechanics**
Editor: T. Schanz

113 **Theoretical and Numerical Unsaturated Soil Mechanics**
Editor: T. chanz

114 **Advances in Medical Engineering**
Editor: Thorsten M. Burzug

115 **X-Ray Lasers 2006**
Proceedings of the 10th International Conference, August 20–25, 2006, Berlin, Germany
Editors: P.V. Nickles, K.A. Januelewicz

116 **Lasers in the Conservation of Artworks**
LACONA VI Proceedings, Vienna, Austria, September 21–25, 2005
Editors: J. Nimmrichter; W. Kautek; M. Schreiner

117 **Advances in Turbulence XI**
Proceedings of the 11th EUROMECH European Turbulence Conference, June 25-28, 2007, Porto, Portugal
Editors: J. M. L. M. Palma; A. Silva Lopes

118 **The Standard Model and Beyond**
Proceedings of the 2nd Int. Summer School in High Energy Physics, Mugla, 25–30 September 2006
Editors: T. Aliev; N.K Pak; M. Serin

119 **Narrow Gap Semiconductors 2007**
Proceedings of the 13th International Conference, 8-12 July, 2007, Guildford, UK
Editors: B.N. Murdin; S.K. Clowes

120 **Microscopy of Semiconducting Materials 2007**
Proceedings of the 15th Conference, 2-5 April, 2007, Cambridge, UK
Editors: A.G. Cullis; P.A. Midgley

Volumes 69–95 are listed at the end of the book.

A.G. Cullis P.A. Midgley
(Eds.)

Microscopy of Semiconducting Materials 2007

Proceedings of the
15th Conference,
2–5 April, 2007, Cambridge, UK

Prof. A.G. Cullis
Department of Electronic and Electrical Engineering
University of Sheffield
Mappin Street
Sheffield S1 3JD
UK

Prof. P.A. Midgley
Department of Materials Science and Metallurgy
University of Cambridge
Pembroke Street
Cambridge CB2 3QZ
UK

Library of Congress Control Number: 2008929346

ISSN 0930-8989
ISBN-13 978-1-4020-8614-4 (HB)
ISBN-13 978-1-4020-8615-1 (e-book)

Published by Springer,
P.O. Box 17, 3300 AA Dordrecht, The Netherlands
In association with
Canopus Publishing Limited,
27 Queen Square, Bristol BS1 4ND, UK

www.springer.com and www.canopusbooks.com

All Rights Reserved
© 2008 Springer Science+Business Media B.V.
No part of this work may be reproduced, stored in a retrieval system, or transmitted in any form or by any means, electronic, mechanical, photocopying, microfilming, recording or otherwise, without written permission from the Publisher, with the exception of any material supplied specifically for the purpose of being entered and executed on a computer system, for exclusive use by the purchaser of the work.

SPRINGER PROCEEDINGS IN PHYSICS

69 **Evolution of Dynamical Structures in Complex Systems**
Editors: R. Friedrich and A.Wunderlin

70 **Computational Approaches in Condensed-Matter Physics**
Editors: S. Miyashita, M. Imada, and H. Takayama

71 **Amorphous and Crystalline Silicon Carbide IV**
Editors: C.Y. Yang, M.M. Rahman, and G.L. Harris

72 **Computer Simulation Studies in Condensed-Matter Physics IV**
Editors: D.P. Landau, K.K. Mon, and H.-B. Schüttler

73 **Surface Science**
Principles and Applications
Editors: R.F. Howe, R.N: Lamb, and K. Wandelt

74 **Time-Resolved Vibrational Spectroscopy VI**
Editors: A. Lau, F. Siebert, and W.Werncke

75 **Computer Simulation Studies in Condensed-Matter Physics V**
Editors: D.P. Landau, K.K. Mon, and H.-B. Schüttler

76 **Computer Simulation Studies in Condensed-Matter Physics VI**
Editors: D.P. Landau, K.K. Mon, and H.-B. Schüttler

77 **Quantum Optics VI**
Editors: D.F.Walls and J.D. Harvey

78 **Computer Simulation Studies in Condensed-Matter Physics VII**
Editors: D.P. Landau, K.K. Mon, and H.-B. Schüttler

79 **Nonlinear Dynamics and Pattern Formation in Semiconductors and Devices**
Editor: F.-J. Niedernostheide

80 **Computer Simulation Studies in Condensed-Matter Physics VIII**
Editors: D.P. Landau, K.K. Mon, and H.-B. Schüttler

81 **Materials andMeasurements in Molecular Electronics**
Editors: K. Kajimura and S. Kuroda

82 **Computer Simulation Studies in Condensed-Matter Physics IX**
Editors: D.P. Landau, K.K. Mon, and H.-B. Schüttler

83 **Computer Simulation Studies in Condensed-Matter Physics X**
Editors: D.P. Landau, K.K. Mon, and H.-B. Schüttler

84 **Computer Simulation Studies in Condensed-Matter Physics XI**
Editors: D.P. Landau and H.-B. Schüttler

85 **Computer Simulation Studies in Condensed-Matter Physics XII**
Editors: D.P. Landau, S.P. Lewis, and H.-B. Schüttler

86 **Computer Simulation Studies in Condensed-Matter Physics XIII**
Editors: D.P. Landau, S.P. Lewis, and H.-B. Schüttler

87 **Proceedings of the 25th International Conference on the Physics of Semiconductors**
Editors: N. Miura and T. Ando

88 **Starburst Galaxies**
Near and Far
Editors: L. Tacconi and D. Lutz

89 **Computer Simulation Studies in Condensed-Matter Physics XIV**
Editors: D.P. Landau, S.P. Lewis, and H.-B. Schüttler

90 **Computer Simulation Studies in Condensed-Matter Physics XV**
Editors: D.P. Landau, S.P. Lewis, and H.-B. Schüttler

91 **The Dense Interstellar Medium in Galaxies**
Editors: S. Pfalzner, C. Kramer, C. Straubmeier, and A. Heithausen

92 **Beyond the Standard Model 2003**
Editor: H.V. Klapdor-Kleingrothaus

93 **ISSMGE**
Experimental Studies
Editor: T. Schanz

94 **ISSMGE**
Numerical and Theoretical Approaches
Editor: T. Schanz

95 **Computer Simulation Studies in Condensed-Matter Physics XVI**
Editors: D.P. Landau, S.P. Lewis, and H.-B. Schüttler

Preface

This volume contains invited and contributed papers presented at the conference on 'Microscopy of Semiconducting Materials' held at the University of Cambridge on 2-5 April 2007. The event was organised under the auspices of the Electron Microscopy and Analysis Group of the Institute of Physics, the Royal Microscopical Society and the Materials Research Society. This international conference was the fifteenth in the series that focuses on the most recent world-wide advances in semiconductor studies carried out by all forms of microscopy and it attracted delegates from more than 20 countries.

With the relentless evolution of advanced electronic devices into ever smaller nanoscale structures, the problem relating to the means by which device features can be visualised on this scale becomes more acute. This applies not only to the imaging of the general form of layers that may be present but also to the determination of composition and doping variations that are employed. In view of this scenario, the vital importance of transmission and scanning electron microscopy, together with X-ray and scanning probe approaches can immediately be seen. The conference featured developments in high resolution microscopy and nanoanalysis, including the exploitation of recently introduced aberration-corrected electron microscopes. All associated imaging and analytical techniques were demonstrated in studies including those of self-organised and quantum domain structures. Many analytical techniques based upon scanning probe microscopies were also much in evidence, together with more general applications of X-ray diffraction methods. The materials subjected to investigation covered the complete range of elemental and compound semiconductors, often in epitaxial form, with some emphasis on both device-processed materials and finished devices at the state-of-the-art. This Proceedings volume presents work described in all study areas.

Every manuscript submitted for publication in this Proceedings volume has been reviewed by at least two referees and modified accordingly. The editors are very grateful to the following colleagues for their rapid and meticulous reviewing work:

A Andreev, J Arbiol, I Arslan, J S Barnard, H Bender, N Browning, T J Bullough, A Cavallini, M Dahne, C Dieker, M Fay, M Galtrey, M Gass, V Grillo, A Harrison, C J Humphreys, Z Liliental-Weber, H Kirmse, M MacKenzie, J Mardinly, G Moldovan, R T Murray, R Oliver, B Pecz, F Priolo, A Rocher, A Rosenauer, F M Ross, J-L Rouviere, O Schmidt, M Schowalter, B Sieber, J Sloan, E Spiecker,V Stolojan, P Sutter, K Tillmann, C Trager-Cowan, T Walther, E Yakimov, N Zakharov.

It is a pleasure to thank Claire Garland and Jodie Cartwright of the Institute of Physics for their expert assistance in organising the present conference. Also, we are very grateful to Erica Bithell, Jo Sharp and Edmund Ward of Cambridge University for editorial assistance in preparing papers for printing in this Proceedings volume.

A G Cullis
P A Midgley
December 2007

Contents

Preface v

Part I Wide Band-Gap Nitrides

The Puzzle of Exciton Localisation in GaN-Based Structures: TEM, AFM and 3D APFIM Hold the Key
C J Humphreys, M J Galtrey, N van der Laak, R A Oliver, M J Kappers, J S Barnard, D M Graham and P Dawson 3

Elastic Strain Distribution in GaN/AlN Quantum Dot Structures: Theory and Experiment
A Andreev, E Sarigiannidou, E Monroy, B Daudin and J Rouvière 13

Concentration Evaluation in Nanometre-Sized $In_xGa_{1-x}N$ Islands Using Transmission Electron Microscopy
A Pretorius, K Müller, T Yamaguchi, R Kröger, D Hommel and A Rosenauer 17

Optical Properties of InGaN Quantum Dots With and Without a GaN Capping Layer
Q Wang, T Wang, P J Parbrook, J Bai and A G Cullis 21

Strain Relaxation in an AlGaN/GaN Quantum Well System
P D Cherns, C McAleese, M J Kappers and C J Humphreys 25

Characterisation of $In_xAl_{1-x}N$ Epilayers Grown on GaN
T C Sadler, M J Kappers, M E Vickers and R A Oliver 29

Generation of Misfit Dislocations in Highly Mismatched GaN/AlN Layers
J Bai, T Wang, P J Parbrook, K B Lee, Q Wang and A G Cullis 33

InN Nanorods and Epilayers: Similarities and Differences
Z Liliental-Weber, O Kryliouk, H J Park, J Mangum, T Anderson and W Schaff 37

Residual Strain Variations in MBE-Grown InN Thin Films
A Delimitis, Ph Komninou, J Arvanitidis, M Katsikini, S-L Sahonta, E Dimakis, S Ves, E C Paloura, F Pinakidou, G Nouet A Georgakilas and Th Karakostas 41

Growth of c-Plane GaN Films on (100) γ-$LiAlO_2$ by Hydride Vapour Phase Epitaxy
A Mogilatenko, W Neumann, E Richter, M Weyers, B Velickov and R Uecker 45

Interaction of Stacking Faults in Wurtzite *a*-Plane GaN on *r*-Plane Sapphire
R Kröger, T Paskova and A Rosenauer 49

Composite Substrates for GaN Growth
B Pécz, L Tóth, L Dobos, P Bove, H Lahrèche and R Langer 53

GaN Layers Grown by MOCVD on Composite SiC Substrate
L Tóth, L Dobos, B Pécz, M A di Forte Poisson and R Langer 57

An Initial Exploration of GaN Grown on a Ge-(111) Substrate
Y Zhang, C McAleese, H Xiu, C J Humphreys, R R Lieten, S Degroote and G Borghs 61

Electron Microscopy Characterization of a Graded AlN/GaN Multilayer Grown by Plasma-Assisted MBE
G P Dimitrakopulos, Ph Komninou, Th Kehagias, A Delimitis, J Kioseoglou, S-L Sahonta, E Iliopoulos, A Georgakilas and Th Karakostas 65

The Effect of Silane Treatment of $Al_xGa_{1-x}N$ Surfaces
N Ketteniss, M J Kappers, C McAleese and R A Oliver 69

Quantitative Analysis of Deformation Around a Nanoindentation in GaN by STEM Diffraction
K K McLaughlin and W J Clegg 73

Microstructure of (Ga,Fe)N Films Grown by Metal-Organic Chemical Vapour Deposition
T Li, C Simbrunner, A Navarro-Quezada, M Wegscheider, M Quast and A Bonanni 77

Nanostructures on GaN by Microsphere Lithography
W N Ng, K N Hui, X H Wang, C H Leung, P T Lai and H W Choi 81

On the Nature of Eu in Eu-Doped GaN
J S Barnard and Y S Beyer 85

Part II General Heteroepitaxial Layers

Recent Studies of Heteroepitaxial Systems
David J Smith 91

Nitrogen-Enhanced Indium Segregation in (Ga,In)(N,As)/GaAs Multiple Quantum Wells
E Luna, A Trampert, E-M Pavelescu and M Pessa 99

Nanoscale Characterisation of MBE-Grown GaMnN/(001) GaAs
M W Fay, Y Han, S V Novikov, K W Edmonds, B L Gallagher, R P Campion, C R Staddon, T Foxon and P D Brown 103

Antiphase Boundaries in GaAs/Ge and GaP/Si
I Németh, B Kunert, W Stolz and K Volz 107

Investigation of the Local Ge Concentration in Si/SiGe Multi-QW Structures by CBED Analysis and FEM Calculations
E Ruh, G Mussler, E Müller and D Grützmacher 111

Crystal Lattice Defects in MBE Grown Si Layers Heavily Doped with Er
N D Zakharov, P Werner, V I Vdovin, D V Denisov, N A Sobolev and U Gösele 115

Epitaxial (001) Ge on Crystalline Oxide Grown on (001) Si
Ch Dieker, J W Seo, A Guiller, M Sousa, J-P Locquet, J Fompeyrine, Y Panayiotatos, A Sotiropoulos, K Argyropoulos and A Dimoulas 119

Analysis of Ge:Mn Magnetic Semiconductor Layers by XPS and Auger Electron Spectroscopy/Microscopy
Yu A Danilov, E S Demidov, S Yu Zubkov, V P Lesnikov, G A Maximov, D E Nikolitchev and V V Podolskii 123

Reduction of Threading Dislocations in Epitaxial ZnO Films Grown on Sapphire (0001)
Y K Sun, D Cherns, P Heard, R P Doherty, Y Sun and M N R Ashfold 127

Part III High Resolution Microscopy and Nanoanalysis

Progress in Aberration-Corrected High-Resolution Transmission Electron Microscopy of Crystalline Solids
K Tillmann, J Barthel, L Houben, C L Jia, M Lentzen, A Thust and K Urban 133

Strain Measurements in SiGe Devices by Aberration-Corrected High Resolution Electron Microscopy
F Hüe, M J Hÿtch, J-M Hartmann, Y Bogumilowicz and A Claverie 149

(S)TEM Characterisation of InAs/MgO/Co Multilayers
D A Eustace, D W McComb, L Buckle, P Buckle, T Ashley, L J Singh, Z H Barber, A M Gilbertson, W R Branford, S K Clowes and L F Cohen 153

Core Composition of Partial Dislocations in N-Doped 4H-SiC Determined by TEM Techniques, Dislocation Core Reconstruction and Image Contrast Analysis
Michaël Texier, Maryse Lancin, Gabrielle Regula and Bernard Pichaud 157

Three-Dimensional Atom Probe Characterisation of III-Nitride Quantum Well Structures
Mark J Galtrey, Rachel A Oliver, Menno J Kappers, Colin J Humphreys, Debbie J Stokes, Peter H Clifton and Alfred Cerezo 161

Novel Method for the Measurement of STEM Specimen Thickness by HAADF Imaging
V Grillo and E Carlino 165

STEMSIM–a New Software Tool for Simulation of STEM HAADF Z-Contrast Imaging
A Rosenauer and M Schowalter 169

On the Role of Specimen Thickness in Chemistry Quantification by HAADF
V Grillo, E Carlino, G Ciasca, M De Seta and C Ferrari 173

Accurate and Fast Multislice Simulations of HAADF Image Contrast by Parallel Computing
E Carlino, V Grillo and P Palazzari 177

Z-contrast STEM 3D Information by Abel transform in Systems with Rotational Symmetry
V Grillo, E Carlino, L Felisari, L Manna and L Carbone 181

Quantifying the Top-Bottom Effect in Energy-Dispersive X-Ray Spectroscopy of Nanostructures Embedded in Thin Films
T Walther 185

Effect of Temperature on the 002 Electron Structure Factor and its Consequence for the Quantification of Ternary and Quaternary III-V Crystals
T J Titantah, D Lamoen, M Schowalter and A Rosenauer 189

Calculation of Debye-Waller Temperature Factors for GaAs
M Schowalter, A Rosenauer, J T Titantah and D Lamoen 195

The Use of the Geometrical Phase Analysis to Measure Strain in Nearly Periodic Images
J-L Rouviere 199

Cross Section High Resolution Imaging of Polymer-Based Materials
D Delaportas, P Aden, C Muckle, S Yeates, R Treutlein, S Haq and I Alexandrou 203

Part IV Self-Organised and Quantum Domain Structures

Direct Observation of Carbon Nanotube Growth by Environmental Transmission Electron Microscopy
H Yoshida, T Uchiyama and S Takeda 209

Band-Gap Modification Induced in HgTe by Dimensional Constraint in Carbon Nanotubes: Effect of Nanotube Diameter on Microstructure
J Sloan, R Carter, A Vlandas, R R Meyer, Z Liu, K Suenaga, P J D Lindan, G Lin, J Harding, E Flahaut, C Giusca, S R P Silva, J L Hutchison and A I Kirkland 213

Gold Catalyzed Silicon Nanowires: Defects in the Wires and Gold on the Wires
M I den Hertog, J L Rouviere, F Dhalluin, P Gentile, P Ferret, C Ternon and T Baron 217

Electron Microscopy Analysis of AlGaN/GaN Nanowires Grown by Catalyst-Assisted Molecular Beam Epitaxy
L Lari, R T Murray, M Gass, T J Bullough, P R Chalker, C Chèze, L Geelhaar and H Riechert 221

Epitaxial Growth of Single Crystalline GaN Nanowires on (0001) Al_2O_3
Th Kehagias, Ph Komninou, G P Dimitrakopulos, S-L Sahonta, C Chèze, L Geelhaar, H Riechert and Th Karakostas 225

Structural Characterisation of GaP <111>B Nanowires by HRTEM
L S Karlsson, J Johansson, C P T Svensson, T Mårtensson, B A Wacaser, J-O Malm, K Deppert, W Seifert, L Samuelson and L R Wallenberg 229

Structural and Chemical Properties of ZnTe Nanowires Grown on GaAs
H Kirmse, W Neumann, S Kret, P Dłużewski, E Janik, G Karczewski and T Wojtowicz 233

TEM Characterization of ZnO Nanorods
R Divakar, J Basu and C B Carter 237

Semiconducting Oxide Single Nanowire Cathodoluminescence Spectroscopy
L Lazzarini, G Salviati, M Zha and D Calestani 241

Determining Buried Wetting Layer Thicknesses to Sub-Monolayer Precision by Linear Regression Analysis of Series of Spectra
T Walther 247

Transmission Electron Microscopy Study of Sb-Based Quantum Dots
B Satpati, V Tasco, N Deguffroy, A N Baranov, E Tournié and A Trampert 251

TEM Characterization of Self-Organized (In,Ga)N Quantum Dots
H Kirmse, I Häusler, W Neumann, A Strittmatter, L Reißmann and D Bimberg 255

Investigating the Capping of InAs Quantum Dots by InGaAs
S L Liew, T Walther, S Irsen, M Hopkinson, M S Skolnick and A G Cullis 259

Comparing InGaAs and GaAsSb Metamorphic Buffer Layers on GaAs Substrates for InAs Quantum Dots Emitting at 1.55µm
Y Qiu, T Walther, H Y Liu, C Y Jin, M Hopkinson and A G Cullis 263

Structural and Compositional Properties of Strain-Symmetrized SiGe/Si Heterostructures
I M Ross, M Gass, T Walther, A Bleloch, A G Cullis, L Lever, Z Ikonic,
M Califano, R W Kelsall, J Zhang and D J Paul 269

EELS and STEM Assessment of Composition Modulation in InAlAs Tensile Buffer Layers of InGaAs/InAlAs/(100)InP Structures
S Estradé, J Arbiol and F Peiró 273

In situ Observation of the Growth of Tungsten Oxide Nanostructures
D C Cox, V Stolojan, G Chen and S R Silva 277

Gas Sensing Properties of Vapour-Deposited Tungsten Oxide Nanostructures
Y Tison, V Stolojan, P C P Watts, D C Cox, G Y Chen and S R P Silva 281

Morphology of Semiconductor Nanoparticles
J Deneen Nowak and C Barry Carter 285

Part V Processed Silicon and Other Device Materials

Light Emission from Si Nanostructures
F Priolo, G Franzò, A Irrera, F Iacona, S Boninelli, M Miritello, A Canino,
C Bongiorno, C Spinella, D Sanfilippo, G Di Stefano, A Piana and G Fallica 291

Hydrogenated Nanocrystalline Silicon Investigated by Conductive Atomic Force Microscopy
A Cavallini, D Cavalcoli, M Rossi, A Tomasi, B Pichaud, M Texier, A Le Donne,
S Pizzini, D Chrastina and G Isella 301

Structural Characterization of Nanocrystalline Silicon Layers Grown by LEPECVD for Optoelectronic Applications
M Texier, M Acciarri, S Binetti, D Cavalcoli, A Cavallini, D Chrastina,
G Isella, M Lancin, A Le Donne, A Tomasi, B Pichaud, S Pizzini and M Rossi 305

Electron Tomography of Mesoporous Silica for Gas Sensor Applications
E Rossinyol, F Bohils, F Cardoso, H Montón, M Roldán, M Rosado,
A Sánchez-Chardi, O Castell and M D Baró 309

Electron Energy-Loss Spectrum Imaging of an HfSiO High-*k* Dielectric Stack with a TaN Metal Gate
M MacKenzie, A J Craven, D W McComb, C M McGilvery,
S McFadzean and S De Gendt 313

Elemental Profiling of III-V MOSFET High-*k* Dielectric Gate Stacks Using EELS Spectrum Imaging
P Longo, A J Craven, J Scott, M Holland and I Thayne 317

Low-Energy Ion-Beam-Synthesis of Semiconductor Nanocrystals in Very Thin High-k Layers for Memory Applications
C Bonafos, S Schamm, A Mouti, P Dimitrakis, V Ioannou-Sougleridis, G Ben Assayag, B Schmidt, J Becker and P Normand 321

Nucleation, Crystallisation and Phase Segregation in HfO_2 and HfSiO
C M McGilvery, S McFadzean, M MacKenzie, F T Docherty, A J Craven, D W McComb and S De Gendt 325

High Accuracy and Resolution for the Separation of Nickel Silicide Polymorphs by Improved Analyses of EELS Spectra
K Asayama, N Hashikawa, M Kawakami and H Mori 329

TEM Study of Ytterbium Silicide Thin Films
J Deneen Nowak, S H Song, S A Campbell and C B Carter 333

TEM Study of the Silicidation Process in Pt/Si and Ir/Si Structures
A Łaszcz, J Ratajczak, A Czerwinski, J Kątcki, N Breil, G Larrieu and E Dubois 337

The Dielectric Properties of Co-Implanted SiO_2 Investigated Using Spatially-Resolved EELS
V Stolojan, W Tsang and S R P Silva 341

Removing Relativistic Effects in EELS for the Determination of Optical Properties
M Stöger-Pollach, A Laister, P Schattschneider, P Potapov and H J Engelmann 345

Analytical STEM Comparative Study of the Incorporation of Covalent (Ge) or Heterovalent (As) Atoms in Silicon Crystal
R Pantel, L Clement, L Rubaldo, G Borot and D Dutartre 349

Lattice Location Determination of Ge in SiC by ALCHEMI
T Kups, M Voelskow, W Skorupa, M Soueidan, G Ferro and J Pezoldt 353

Part VI Device and Doping Studies

Moore's Law and its Effect on Microscopy in the Semiconductor Industry
John Mardinly 361

Tomographic Analysis of a FinFET Structure
O Richard, A Kalio, H Bender and E Sourty 375

3-D Characterisation of the Electrostatic Potential in an Electrically Biased Silicon Device
A C Twitchett-Harrison, R E Dunin-Borkowski and P A Midgley 379

Three-Dimensional Field Models for Reverse Biased P-N Junctions
F Ubaldi, G Pozzi, P F Fazzini and M Beleggia 383

Automated Quantification of Dimensions on Tomographic Reconstructions of Semiconductor Devices
A Kalio, O Richard, E Sourty and H Bender 387

Dopant Profiling in the TEM: Progress Towards Quantitative Electron Holography
D Cooper, A C Twitchett, P A Midgley and R E Dunin-Borkowski 391

Observation of Dopant Distribution in Compound Semiconductors Using Off-axis Electron Holography
H Sasaki, S Ootomo, T Matsuda, K Yamamoto and T Hirayama 395

Dopant Profiling of Silicon Calibration Specimens by Off-Axis Electron Holography
D Cooper, R Truche, F Laugier, F Bertin and A Chabli 399

Novel Approach for Visualizing Implants in Deep Submicron Microelectronic Devices Using Dopant Selective Etching and Low keV SEM
Y Chakk, I Vidoshinsky and R Razilov 403

Quantitative Dopant Profiling in the SEM Including Surface States
K W A Chee, C Rodenburg and C J Humphreys 407

On the Asymmetric Splitting of CBED HOLZ Lines under the Gate of Recessed SiGe Source/Drain Transistors
A Benedetti and H Bender 411

CBED and FE Study of Thin Foil Relaxation in Cross-Section Samples of $Si/Si_{1-x}Ge_x$ and $Si/Si_{1-x}Ge_x/Si$ Heterostructures
L Alexandre, G Jurczak, C Alfonso, W Saikaly , C Grosjean, A Charaï and J Thibault 415

Stress and Strain Measurement in Stressed Silicon Lines
A Béché, J L Rouvière, J C Barbé, F. Andrieu, D Rouchon, J Eymery and M Mermoux 419

Measuring Strain in Semiconductor Nanostructures by Convergent Beam Electron Diffraction
L Clément, J-L Rouviere, F Cacho and R Pantel 423

Part VII FIB, SEM and SPM Advances

Nano-FIB from Research to Applications - a European Scalpel for Nanosciences
J Gierak, A Madouri, A L Biance, E Bourhis, G Patriarche, C Ulysse, X Lafosse, L Auvray, L Bruchhaus, R Jede and Peter Hawkes 431

Advanced Focused Ion Beam Specimen Preparation for Examination by Off-Axis Electron Holography
D Cooper, R Truche, P A Midgley and R E Dunin-Borkowski 441

Critical Thickness for Semiconductor Specimens Prepared using Focused Ion Beam Milling
A C Twitchett-Harrison, R E Dunin-Borkowski and P A Midgley 445

Organic-Based Micropillar Structure Fabrication by Advanced Focused Ion Beam Milling Techniques
Wen-Chang Hung, Ali M Adawi, Ashley Cadby, Liam G Connolly, Richard Deanl Abbes Tahraoui, A M Fox, David G Lidzey and A G Cullis 449

Controlled Band Gap Modulation of Hydrogenated Dilute Nitrides by SEM-Cathodoluminescence
G Salviati, L Lazzarini, N Armani, M Felici, A Polimeni, M Capizzi, F Martelli, S Rubini and A Franciosi 453

Interdiffusion as the First Step of GaN Quantum Dot Degradation Demonstrated by Cathodoluminescence Experiments
B Sieber 459

Calibration and Applications of Scanning Capacitance Microscopy: n-Type GaN
J Sumner, R A Oliver, M J Kappers and C J Humphreys 463

The Factors Influencing the Stability of Scanning Capacitance Spectroscopy
Mao-Nan Chang, Tung-Huan Chou, Che-Yu Yang and Jeng-Hung Liang 467

Growth and *in vivo* STM of III-V Compound Semiconductors
F Bastiman, A G Cullis, M Hopkinson and M Green 471

Mapping Defects in Dielectrics with Dynamic Secondary Electron Contrast in the low Vacuum SEM
Brad Thiel 477

EBIC Characterization of Light Emitting Structures Containing InGaN/GaN MQW
E B Yakimov 481

EBIC Characterisation of Diffusion and Recombination of Minority Carriers in GaN-Based LEDs
G Moldovan, V K S Ong, O Kurniawan, P Kazemian, P R Edwards and C J Humphreys 485

A Parametric Study of a Diode-Resistor Contrast Model for SEM-REBIC of Electroceramics
A G Wojcik and L E Wojcik 489

Author Index 491

The Puzzle of Exciton Localisation in GaN-Based Structures: TEM, AFM and 3D APFIM Hold the Key

C J Humphreys, M J Galtrey, N van der Laak, R A Oliver, M J Kappers, J S Barnard, D M Graham[1] and P Dawson[1]

Department of Materials Science and Metallurgy,University of Cambridge, Pembroke Street, Cambridge, CB2 3QZ, UK
[1]School of Physics and Astronomy, University of Manchester, Manchester, M60 1QD, UK

Summary: The InGaN/GaN quantum well system emits intense light even though the dislocation density is high. This is a puzzle since dislocations should quench the light emission. Photoluminescence (PL) experiments show that the excitons in the InGaN quantum well are localised on a nanometre scale, thus separating the carriers from most of the dislocations. Many papers report transmission electron microscopy (TEM) results showing that this localisation is caused by gross indium clustering in the InGaN quantum wells, but our TEM reveals no gross indium clustering. Three-dimensional atom probe field ion microscopy confirms that InGaN is a random alloy. Mechanisms are given for localisation on a nm scale. Confinement on a broader length scale (50 – 100 nm) can also occur in some InGaN quantum wells.

1 Introduction

A remarkable feature of InGaN/GaN quantum well LEDs is that they emit intense light, even though the dislocation density is typically 10^9cm^{-2}. In all other light-emitting semiconductors the light emission is quenched if the dislocation density exceeds about 10^3cm^{-2}. Yet InGaN quantum wells emit strong blue and green light (depending on the In concentration) when the dislocation density is one million times higher than that in other light-emitting semiconductors, even though it is known that dislocations in InGaN are non-radiative recombination centres.

The widely-believed solution to the above problem, up to a few years ago, was that InGaN was an unstable alloy and the indium in the InGaN quantum wells formed In-rich clusters. Since the band-gap of InN is less than that of GaN, the bandgap of these In-rich clusters is reduced, and hence the electrons and holes are spatially localised in these clusters. At room temperature (and below) in InGaN, an electron and hole form a bound exciton, hence the In-rich clusters localise the excitons. The clusters were believed to be small, on a nanometre scale. Statistically, most threading dislocations would not pass through these nanometre-scale In-rich clusters, even for a dislocation density of 10^9cm^{-2} at which the average dislocation spacing is about 300 nm. Hence it was almost universally believed that the In-rich clusters localised the excitons away from most of the dislocations so that they did not quench the light emission. Thus it was believed that the intense light emission observed from InGaN quantum wells with a high dislocation density was due to In-rich clusters.

In this paper we first present evidence to support this argument. We then show that In-rich clusters are produced in InGaN in the electron microscope due to electron beam damage. However, careful low-dose electron microscopy reveals no gross In clustering, but it cannot rule out small In fluctuations. We then report that three-dimensional atom probe analysis of InGaN quantum wells yields that InGaN is a random alloy, with no In fluctuations other than would be expected of any random alloy. This is consistent with our electron microscopy results. Finally, we return to the question of why InGaN emits intense light despite having a high dislocation density.

2 The Evidence for Exciton Localisation in InGaN

There is clear evidence that, at low temperature, the dominant emission from InGaN/GaN quantum-well structures involves the recombination of strongly localised excitons (see, for example [1, 2]). Graham et al [2] studied the low temperature (T = 6 K) optical properties of a series of $In_xGa_{1-x}N$/GaN single-quantum-well structures where the indium fraction x varied from sample to sample over the range 0.05 – 0.25. The structures were grown by Metal Organic Vapour Phase Epitaxy (MOVPE), and the InGaN quantum well was 2.5 nm thick. By comparing the strengths of the phonon-accompanied recombination with those obtained from a theoretical model, the spatial extent of the carrier wavefunctions in the plane of the quantum well was estimated. This localisation length was found to range from 1 nm for the InGaN quantum well containing 25% indium, to 3 nm for the 5% indium alloy. Thus the exciton localisation length in the plane of the quantum well is typically about 2 nm. The key question is what causes this localisation.

3 The Evidence from Electron Microscopy for Indium-Rich Clusters

Bright-field transmission electron microscopy (TEM) images of InGaN/GaN quantum well structures were reported to show dark dot-like features with a size of about 3 nm in the InGaN quantum wells [3, 4]. Since an indium atom is much larger than a gallium atom, fluctuations in InGaN compositions will cause variations in lattice strain and hence strain contrast in TEM images. The dot-like features were therefore attributed to strain contrast. Energy-dispersive X-ray analysis in the TEM suggested a correlation between the dark spots and higher indium content [4]. This was confirmed by Cho et al [5] who used energy-filtered transmission electron microscopy (EFTEM) to analyse the regions of strain contrast observed in InGaN quantum wells. EFTEM images clearly revealed these strained regions to be indium-rich clusters with a size of 2-3 nm.

A popular method for studying these indium-rich clusters has been lattice parameter mapping. In this technique, high-resolution TEM lattice images are taken of InGaN/GaN quantum well structures. The indium-rich clusters give rise to localised strain, and by measuring the local lattice fringe spacings a two-dimensional lattice parameter map can be plotted, which shows the size of the indium-rich clusters to be typically a few nm. Strains of the order of 10% are found in these clusters. By using Vegard’s law, the lattice parameter map can be converted to a composition map. For InGaN quantum wells grown with 10-20% indium, the indium-rich clusters are typically found to contain at least 80% indium [6, 7], although the projection problem in TEM makes it difficult to quantify the indium content. We will call such clusters “gross indium-rich clusters”. It was reported that such gross indium-rich clusters may, in fact, be pure InN [7], and pure InN regions with a 1-3 nm size were reported in InGaN quantum wells grown by both MOVPE and MBE, as measured using high resolution TEM lattice parameter mapping of samples with mean composition of 16% In in the InGaN quantum wells [8].

The argument for gross indium clustering in InGaN quantum wells appears to be strong. We know from optical measurements that the excitons in InGaN are localised on a 1-3 nm scale. Thermodynamic calculations show that InGaN is unstable and should decompose into In-rich and In-poor regions [9]. TEM shows gross In-rich clusters in InGaN quantum wells on a nanometre scale, similar to the scale on which the excitons are localised.

Because of the apparently strong and convincing arguments given above, many hundreds of papers have been published stating that InGaN quantum wells contain gross In-rich clusters, and that these clusters are responsible for the exciton localisation. The Cambridge GaN research group has observed such clusters in the TEM many times, and indeed they are among the authors of a paper demonstrating that those clusters are indium-rich [5]. However, this work necessarily used high electron doses for the EFTEM images which revealed the In-rich clusters. We will now demonstrate that in the wide range of InGaN materials we have examined, such gross indium-rich clusters do not exist, and they are produced by electron beam damage in the TEM.

4 The Effect of Electron Beam Damage on InGaN in the TEM

We have found that InGaN quantum wells damage extremely rapidly in the electron beam of a TEM at the beam currents normally used for imaging. The damage causes indium-rich clusters to form. Figure 1 shows (0002) lattice fringe images of an $In_{0.22}Ga_{0.78}N$ quantum well using high-resolution TEM (HRTEM). The lattice fringe images were obtained with the specimen tilted about 6-7 deg away from a <11$\bar{2}$0> axis towards the adjacent <10$\bar{1}$0> pole. At this orientation a systematic row of reflections are excited with (0002) and (000$\bar{2}$) under equal excitation. The images in Fig. 1 were recorded using 400 keV incident electrons in a JEOL 4000EX. Figure 1a was recorded within 20 seconds of first exposing this part of the quantum well to the electron beam. Figure 1b is the same area after a few minutes of exposure. We have analysed these images to produce lattice parameter maps [10, 11] using a process similar to the DALI technique [7]. After only a few minutes exposure to the electron beam we found nanometre-size indium clusters formed which caused local strains of up to 10%, corresponding to an indium fraction x of 60%. These cluster sizes, strains and compositions are typical of those found by others using TEM (for example [6, 7]). However, we have found no evidence at all of gross indium clustering if low electron beam currents are used. At low electron dose, the lattice fringe image of the quantum well and the lattice parameter map are both reasonably uniform (Fig. 1a, 1c), [10, 11]. We have studied the effect of 200, 300, and 400 keV incident electrons. For the 200 keV electrons we used a FEI Tecnai F20-G2. We reduced the electron beam current substantially below the maximum available, so that the current density incident on the sample was $35 Acm^{-2}$. Electron beam damage of the InGaN QWs was already strong after less than 30 seconds of exposure to 200 keV electrons at this current density.

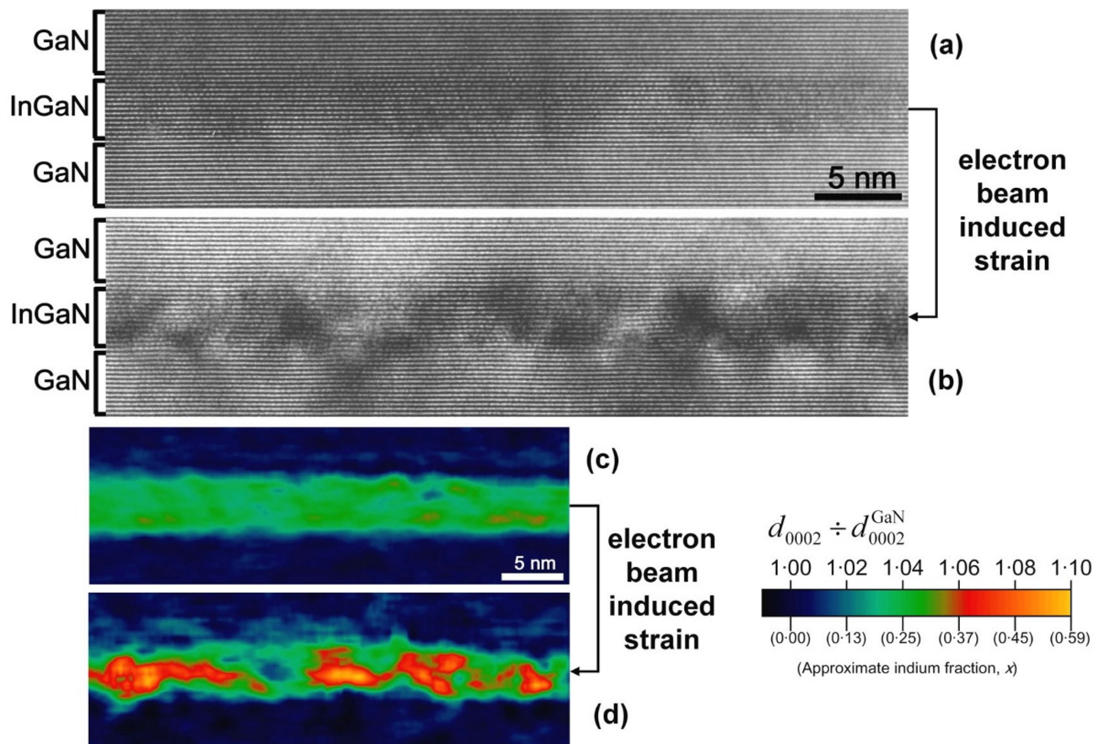

Fig. 1. A pair of HRTEM lattice fringe images demonstrating the electron-beam induced damage to an $In_{0.22}Ga_{0.78}N$ quantum well. The (0002) lattice fringe images were obtained using a JEOL 4000 EX operating at 400kV. (a) shows the image after minimal exposure to the beam, and (b) the same region after only a few minutes of exposure. (c) is a lattice parameter map of (a), and (d) is a lattice parameter map of (b).

Since publishing the Smeeton et al [10, 11] papers it has been suggested to us that our results may apply only to InGaN grown on MOVPE equipment at Cambridge, or may be related to our TEM specimen preparation procedures, rather than being a general effect. We have therefore purchased a very bright blue commercial LED and examined the InGaN quantum wells it contains by TEM. Again, we found no evidence of gross indium clustering at low electron beam currents and short exposure times in the TEM. However, as the electron dose increased, indium-rich clusters formed, just as in the Cambridge grown samples [12]. O'Neill et al [13] also reported that In-rich clusters formed as a result of electron beam damage in their specimens. We also prepared TEM specimens using only mechanical polishing instead of using a combination of mechanical polishing followed by ion beam thinning. We observed no differences in the behaviour of both specimens in the TEM, suggesting that the susceptibility of InGaN to electron beam damage is intrinsic to the InGaN/GaN system and not a consequence of our ion milling procedures [12]. We have also studied MBE grown InGaN/GaN structures. In *all* the samples we have studied, we observe no gross indium clustering in the TEM at low beam currents and short exposure times. Indium-rich clusters *only* appear at higher electron doses.

5 Does TEM Give Any Evidence for Genuine In Clustering?

Slight fluctuations in the TEM image contrast of InGaN quantum wells can be observed in low-dose images. It should be noted that if InGaN is a random alloy, the composition will not be uniform and some statistical fluctuations will be observed. Hence, the small fluctuations that are observed in TEM image contrast could be due to random alloy fluctuations or to genuine low-level In-clustering. In addition, the initial stages of damage may already have occurred in low-dose images, since significant radiation damage can occur in orienting the specimen in the electron microscope before recording the image. Hence even the lowest dose images should not be treated as a faithful representation of the original specimen.

In the light of the Smeeton et al [10, 11] papers, which suggested that the gross indium-rich clusters in InGaN quantum wells reported by many researchers might be due to electron beam damage, the Gerthsen group revised their earlier conclusions [7]. They observed that the indium concentration in the clusters increased with increasing irradiation time in the electron microscope. However, because they found In-rich clusters already in their first HRTEM images taken after only 20s of exposure to the electron beam they concluded that In-rich clusters genuinely existed in their InGaN quantum wells, but that the In concentration was significantly lower than they had previously stated [14].

The Kisielowski group has recently made detailed studies of indium clustering in InGaN, following their earlier work [6]. They claim that InGaN quantum wells can be imaged in HRTEM with negligible electron beam damage and that indium-rich clusters genuinely exist [15]. They have found that no measurable alteration of the initial element distribution occurs for electron irradiation times of up to 2 minutes and current densities of 20-40 Acm^{-2} [16]. They report that green $In_xGa_{1-x}N$ quantum wells (with average indium fraction x about 0.2) have genuine indium-rich clusters, 1-3 nm wide with In content up to 0.40 [17]. This disagrees with our findings reported above (see Fig. 1).

A key question is whether the electron micrographs carefully recorded and reported in the above papers [14-17] are, in fact, damage free. Electron-beam damage of inorganic materials in an electron microscope can be a complex process and the damage mechanism for strained thin layers of InGaN is not yet known. In some inorganic materials, there appears to be a threshold electron beam current density for damage to occur, below which there appears to be little or no damage [18, 19]. If InGaN behaves in this way then Gerthsen and Kisielowski may be correct that damage-free electron micrographs of this material can be recorded. However, for other inorganic materials there appears to be no lower threshold electron beam current density for damage, which can also occur for incident electron energies as low as 40 keV [20]. If InGaN behaves in this way then damage-free microscopy is impossible. Until more is

known about the mechanism(s) by which strained thin layers of InGaN damage, we cannot be sure that it is possible to record high resolution electron micrographs in which the damage is negligible.

6 3-D Atom Probe Studies of Indium Clustering

Our low-dose TEM studies have revealed that gross indium clustering does not exist in the many InGaN quantum wells we have studied. However, we cannot rule out lower level indium clustering for the reasons given above, namely the fact that such genuine clustering, if it exists, may be masked by the noise in low-dose images, and genuine clusters cannot be distinguished from indium-rich clusters already created by the electron beam in even low-dose images. In addition, since the electron-beam damage mechanism in strained layers of InGaN is not yet known, we do not know if it is possible to record damage-free electron micrographs of this material. In order to assess whether low-level indium clustering genuinely exists we therefore need a different technique from electron microscopy. The method should not involve exposure to high-energy electrons, and it should preferably provide direct information, at the atomic level, of the distribution of indium in InGaN quantum wells. In addition, the technique should preferably avoid the projection problem in TEM.

It is well known that the three-dimensional atom probe (3DAP) can provide nanometre-scale information about composition variations in a variety of materials [21]. We have recently applied this technique to InGaN quantum wells. Needle-shaped 3DAP specimens were prepared in a FEI Dualbeam Quanta FIB/SEM. All SEM imaging was performed at 5 kV and exposure times and currents were minimised in order to limit the risk of damage to the InGaN quantum wells. The 3DAP images were obtained using an Oxford nanoScience instrument fitted with a prototype laser module.

Figure 2 shows reconstructions of the InGaN/GaN structure with the indium and gallium atoms displayed. Four indium-containing quantum wells are clearly visible, and we have analysed in detail the indium distribution in the bottom three of these since the top well may have been damaged by sample preparation. We have compared the indium distribution with the expected distribution from a random alloy. No significant deviations were found from that expected in a random alloy for all three of the quantum wells (for further details see [22, 23]. We therefore conclude that there is no evidence of indium clustering in this sample.

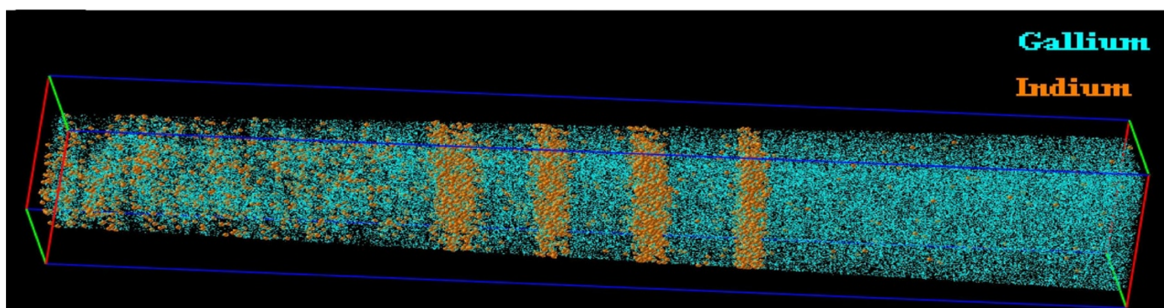

Fig. 2. Three-dimensional Atom Probe Field Ion Microscope (3DAP) image of InGaN/GaN multi-quantum wells. Each dot represents a single atom: light blue is gallium and orange is indium. Statistical analysis shows that the indium distribution is as expected in a random alloy.

Two independent direct imaging techniques, TEM and 3DAP, have therefore found no evidence for indium clustering in InGaN quantum wells. The 3DAP results indicate that the distribution of indium in the InGaN sample studied is that of a random alloy. Local compositional fluctuations statistically exist of course in a random alloy, but there is no atomic clustering.

7 Localisation Mechanisms

The evidence for exciton localisation on a nanometre scale in InGaN quantum wells is strong (see Section 2). This is consistent with InGaN quantum well structures emitting intense light with high quantum efficiency, despite having a high dislocation density. In this section we discuss possible mechanisms for the carrier localisation, having ruled out gross indium clustering.

7.1 Quantum Well Thickness Fluctuations

At low temperature, excitons are known to be localised in GaAs/AlGaAs quantum wells by well-width fluctuations. The localisation energy is typically only a few meV, and so localisation by this mechanism only occurs at low temperature in GaAs/AlGaAs [24]. However, the localising effects of well-width fluctuations are much greater in the InGaN/GaN quantum-well system, both because the InGaN is more highly strained and because the piezoelectric effect is much stronger than in GaAs/AlGaAs.

High-resolution electron micrographs show that in the InGaN/GaN quantum well system, the lower quantum well interface appears to be atomically abrupt, whereas the upper interface is atomically rough [2]. The in-plane extent of these well-width fluctuations is small, typically a few nm. The thickness variation is typically one monolayer (= 0.259 nm). Calculations show that for an InGaN/GaN quantum well system with an indium fraction of 0.25, and well widths of 3.3 nm and 3.3 nm + 1 monolayer, the quantum well bandgap for the n = 1 electron and hole confined states decreases by 58 meV. Since kT at room temperature is 25 meV, a monolayer change in quantum well thickness, consistent with electron micrographs, is sufficient to localise the carriers [2].

7.2 Indium-Localised Hole Wave Functions

Bellaiche et al [25] have suggested from theoretical calculations of cubic InGaN that even for a perfectly homogeneous InGaN material the carriers could be localised. The calculations predict localisation of the hole wavefunctions around indium in InGaN along randomly formed In-N-In chains. Hole localisation leads to exciton localisation because of the small effective Bohr radius of excitons in GaN (= 3.4 nm). Chichibu et al [26] have recently explained their positron annihilation results in InGaN in terms of such In-N-In chains. Unfortunately there is no theoretical calculation of the carrier localisation energy due to In-N-In chains in a random hexagonal InGaN alloy.

8 Thermodynamics of Strained InGaN

The thermodynamic calculations reported earlier [9] which predicted the decomposition of InGaN were for bulk material. However Karpov [27] has calculated the phase diagram for an InGaN layer epitaxially matched to a GaN layer, which puts the InGaN into biaxial compression. The effect of the strain is to stabilise the InGaN, and no decomposition is predicted for normal growth conditions.

Electron microscopy of the InGaN quantum wells we have studied in this paper reveals no misfit dislocations. We are aware that the measured critical thickness for the introduction of misfit dislocations depends on the resolution of the experimental technique used to detect the dislocations [28] and that electron microscopy, because of the limited volume of specimen sampled, may over-estimate the critical thickness. However, electron microscopy indicates that, at least locally, our InGaN quantum wells are fully strained, and this is confirmed by our X-ray diffraction measurements.